



Near-field time-reversal amplification

Stephane G Conti, Philippe Roux, William A Kuperman

► To cite this version:

Stephane G Conti, Philippe Roux, William A Kuperman. Near-field time-reversal amplification. Journal of the Acoustical Society of America, 2007, 121, <10.1121/1.2724238>. <hal-04028117>

HAL Id: hal-04028117

<https://hal.science/hal-04028117v1>

Submitted on 14 Mar 2023

HAL is a multi-disciplinary open access archive for the deposit and dissemination of scientific research documents, whether they are published or not. The documents may come from teaching and research institutions in France or abroad, or from public or private research centers.

L'archive ouverte pluridisciplinaire **HAL**, est destinée au dépôt et à la diffusion de documents scientifiques de niveau recherche, publiés ou non, émanant des établissements d'enseignement et de recherche français ou étrangers, des laboratoires publics ou privés.



HAL Authorization

See discussions, stats, and author profiles for this publication at: <https://www.researchgate.net/publication/6283418>

Near-field time-reversal amplification

Article in *The Journal of the Acoustical Society of America* · July 2007

DOI: 10.1121/1.2724238 · Source: PubMed

CITATIONS

51

READS

189

3 authors, including:



Philippe Roux

University Grenoble Alpes

494 PUBLICATIONS 12,948 CITATIONS

SEE PROFILE

Some of the authors of this publication are also working on these related projects:



Seismic tomography of the San Jacinto Fault zone [View project](#)



Array processing based on high-order statistics [View project](#)

Near-field time-reversal amplification

Stephane G. Conti,^{a)} Philippe Roux, and William A. Kuperman

Marine Physical Laboratory, SIO-UCSD, 9500 Gilman Drive, La Jolla, California 92093-0238

(Received 13 December 2006; revised 14 March 2007; accepted 19 March 2007)

The spatial resolution of the focused field of a classical time-reversal mirror has a wavelength-order λ diffraction limit. Previously reported results for subwavelength focus require either the full knowledge of the original source or the evanescent waves in the near field. Here it is shown that subwavelength focusing can be achieved without *a priori* knowledge of the original probe source. If the field is recorded at a few wavelengths away from the probe source, where the amplitude of the near field is too low for subwavelength focusing, it is shown that the low amplitude near field can be amplified and the spatial resolution improved, using the near-field time reversal (NTR) procedure introduced here. The NTR is performed from the phase of the spatial spectrum of the field recorded on an array around the original probe source using an analytical continuation for the amplitude of the spatial spectrum. Following theory, $\lambda/20$ resolution is experimentally demonstrated with audible acoustic wavefields in the air. © 2007 Acoustical Society of America. [DOI: 10.1121/1.2724238]

PACS number(s): 43.60.Tj, 43.20.Gp, 43.28.Hr, 43.60.Sx [EJS]

Pages: 3602–3606

I. INTRODUCTION

The implementation of a time-reversal mirror (TRM) in acoustics¹ and electromagnetics^{2–4} is now well established. Using the far field of a probe source, a TRM focuses back to the probe to the wavelength (λ) diffraction resolution^{5,6} as determined by the TRM aperture.^{6–8} Previous studies^{5,9} showed that the field resulting from the time reversal process near the focus consists of two waves: the incoming wave from the TRM and the outgoing wave after the collapse of the time-reversed field at the source. Using Lamb waves on a chaotic glass plate cavity, de Rosny and Fink⁹ showed that subwavelength spatial resolution could be achieved experimentally by active cancellation of the outgoing wave at the source location at precisely the right time and amplitude as specified by the time-reversal process. This acoustic sink is implemented by adding a wave emitted from a time-reversed source, ϕ_S , to the field traveling from the TRM, ϕ_{TR} . In other words, the acoustic sink combines the *a priori* knowledge of the original source position with the far-field time-reversal data. On the other hand, near-field acoustic holography (NAH)^{10,11} utilizes the evanescent wave-number structure of the nearfield for the high resolution characterization without *a priori* knowledge of the source. In this paper, we introduce a near-field time-reversal (NTR) procedure that combines the acoustic sink and NAH approaches. We show that a focus with subwavelength resolution can be obtained from a TRM at a distance of a few wavelengths of the probe source, between the near- and far-field regions. Importantly, the subwavelength focusing is achieved without *a priori* knowledge of the original source position and timing. This result is obtained in the wave-number domain from the spatial spectrum of the field ϕ_{TR} recorded with an array around the probe source. If the range is of the order of a few wavelength, the amplitude of the evanescent field is too low for subwavelength resolution focusing like in the nearfield. Nevertheless,

part of the evanescent field can be amplified in the wave-number domain to significantly improve the resolution of the focus. Here, we demonstrate this principle using simulation and experiments for a range of 4 wavelengths. The NTR procedure we propose consists in extracting the phase of the time-reversed field in the wave-number domain and applying a generic amplitude to the spectrum while retaining the recorded phase.

II. THEORY

Time reversal is always implemented directly in the spatial domain whereas NAH uses the wave-number domain to reconstruct the field at the source. Near-field Time Reversal (NTR) takes advantages of the fact that in the wave-number domain, the near field of a point source ϕ_S is decomposed into an amplitude that controls the spatial resolution of the focus independent of its position and a phase that contains the spatial position information of the focus. In our case, the latter can also be extracted from the time-reversed signals ϕ_{TR} recorded around the source. The amplitude and the phase can be combined because the near-field spatial resolution is independent of the probe source position. The resulting constructed near-field time-reversal (NTR) focus occurs at the position in space and time defined by the TRM but with the spatial resolution one expects from the nearfield. The temporal resolution of the focus remains unchanged.

In other words, Near-field time reversal at the source position $\mathbf{R}_1 = (x_1, y_1, z_1)$ is based on the combination of two fields on a near-field array \mathbf{R} around the source. First, as usual in a time-reversal process, after the field from the source is recorded away from the nearfield on a multiple-element array that makes up a TRM, the transmitted time-reversed field $\phi_{TR}(\mathbf{R}, \mathbf{R}_1, t)$ focusing to the probe source position with a wavelength-order spatial resolution is recorded on the near-field array. Second, we define the generic analytic field $\phi_S(\mathbf{R}, \mathbf{R}_0, t)$ for an isotropic point source in free space at position \mathbf{R}_0 as the target field for the time-reversed imaging. This field $\phi_S(\mathbf{R}, \mathbf{R}_0, t)$ defines the subwavelength

^{a)}Electronic mail: scont@ucsd.edu

spatial resolution to achieve. As it will be shown later, the same generic field $\phi_S(\mathbf{R}, \mathbf{R}_0, t)$ is applied to a time-reversed field from one source or two simultaneous ones separated by less than a wavelength. In both cases, this generic field will provide resolvable foci at the original positions. Note that \mathbf{R}_0 and \mathbf{R}_1 do not need to be the same point for ϕ_S and ϕ_{TR} , meaning that the NTR procedure is applied without *a priori* knowledge on the position of the focus from the TRM. For $|\mathbf{R}_0 - \mathbf{R}| < \lambda$, $\phi_S(\mathbf{R}, \mathbf{R}_0, t)$ is given⁹

$$\phi_S(\mathbf{R}, \mathbf{R}_0, t) = A_S \frac{\exp(ik_0|\mathbf{R} - \mathbf{R}_0|)}{4\pi|\mathbf{R} - \mathbf{R}_0|} \exp(-i\omega t), \quad (1)$$

where $k_0 = \omega/c = 2\pi f_0/c$ for the central frequency f_0 , c is the speed of sound, and A_S is the relative amplitude of the field ϕ_S . The spatial resolution for $\phi_S(\mathbf{R}, \mathbf{R}_0, t)$ corresponds to a point source. For a position \mathbf{R}_1 in the nearfield of the probe source such that $|\mathbf{R}_1 - \mathbf{R}| < \lambda$, and a TRM in the farfield of the probe source, the time-reversed field from the farfield $\phi_{TR\,ff}(\mathbf{R}, \mathbf{R}_1, t)$ is given by⁹

$$\begin{aligned} \phi_{TR\,ff}(\mathbf{R}, \mathbf{R}_1, t) = & A_{TR} \frac{\exp(-ik_0|\mathbf{R} - \mathbf{R}_1|)}{4\pi|\mathbf{R} - \mathbf{R}_1|} \exp(-i\omega t) \\ & - A_{TR} \frac{\exp(ik_0|\mathbf{R} - \mathbf{R}_1|)}{4\pi|\mathbf{R} - \mathbf{R}_1|} \exp(-i\omega t), \quad (2) \end{aligned}$$

where A_{TR} the relative amplitude of the field $\phi_{TR\,ff}$. If the TRM is in a range between the farfield and the nearfield of the probe source, the time-reversed field recorded on the near-field array is the sum of the fields from Eqs. (1) and (2), with relative amplitudes A_S and A_{TR} varying with the range:

$$\phi_{TR}(\mathbf{R}, \mathbf{R}_1, t) = \phi_{TR\,ff}(\mathbf{R}, \mathbf{R}_1, t) + \phi_S(\mathbf{R}, \mathbf{R}_1, t). \quad (3)$$

As in Eq. (3), for a TRM in the nearfield, the relative amplitudes A_S and A_{TR} are equal, and $\phi_{TR}(\mathbf{R}, \mathbf{R}_1, t)$ describes the focus whose spatial resolution corresponds to a point source. For a TRM in the farfield, A_S is equal to zero, and the spatial resolution is of the order λ corresponding to the sinc function for an ideal TRM in the farfield. Note that Eqs. (1)–(3) only require the medium to be locally homogeneous around the source. In this case, the time-reversed field obtained on the near-field array does not depend on the presence of scatterers or heterogeneities at distances greater than a few wavelengths between the TRM and the source. However, when an ideal TRM is not available, scatterers or heterogeneities can increase the effective aperture of the TRM,^{6–8} making the time-reversed field behave as $\phi_{TR}(\mathbf{R}, \mathbf{R}_1, t)$ around the source. Following Eqs. (1) and (2), ϕ_S and ϕ_{TR} are written as the product of space $g_S(\mathbf{R}, \mathbf{R}_0)$ and $g_{TR}(\mathbf{R}, \mathbf{R}_1)$, respectively, and a time dependent function $\exp(-i\omega t)$:

$$\phi_S(\mathbf{R}, \mathbf{R}_0, t) = A_S g_S(\mathbf{R}, \mathbf{R}_0) \exp(-i\omega t), \quad (4)$$

$$\phi_{TR}(\mathbf{R}, \mathbf{R}_1, t) = A_{TR} g_{TR}(\mathbf{R}, \mathbf{R}_1) \exp(-i\omega t). \quad (5)$$

The localization of the time-reversed wave at the original source position is embedded in $g_{TR}(\mathbf{R}, \mathbf{R}_1)$. In the wave-number domain, the localization of the original source only appears in the phase term, by definition of the Fourier trans-

form. In the near field, the spatial Fourier transform $\tilde{\phi}$ of either Eq. (1) or (3) is written as

$$\tilde{\phi}_S(\mathbf{k}, \mathbf{R}_1, t) = A_S \exp(-i\mathbf{k} \cdot \mathbf{R}_0) \tilde{g}_S(\mathbf{k}) \exp(-i\omega t), \quad (6)$$

$$\tilde{\phi}_{TR}(\mathbf{k}, \mathbf{R}_1, t) = A_{TR} \exp(-i\mathbf{k} \cdot \mathbf{R}_1) \tilde{g}_{TR}(\mathbf{k}) \exp(-i\omega t). \quad (7)$$

The space dependent functions $\tilde{g}_S(\mathbf{k})$ and $\tilde{g}_{TR}(\mathbf{k})$ of the spatial Fourier transforms of ϕ_S and ϕ_{TR} act as the shaping filter of the focus. They are independent of the source localization \mathbf{R}_0 and \mathbf{R}_1 , respectively. Equation (7) confirms that the focal position in $\tilde{\phi}_{TR}(\mathbf{k}, \mathbf{R}_1, t)$ is only present in the phase term $\exp(-i\mathbf{k} \cdot \mathbf{R}_1)$, while Eqs. (6) and (7) confirm that $\tilde{g}_S(\mathbf{k})$ and $\tilde{g}_{TR}(\mathbf{k})$ contain the near-field spatial information of $\phi_S(\mathbf{k}, \mathbf{R}_0, t)$ and $\phi_{TR}(\mathbf{k}, \mathbf{R}_1, t)$, respectively. With a TRM in the farfield, the localization phase $\exp(-i\mathbf{k} \cdot \mathbf{R}_1)$ is present in the spectrum for $k \leq k_0$, and also for $k > k_0$ when the TRM is in the nearfield. For a TRM at a distance in between these two regimes, the localization phase is present for all values of the wave number k , even if the corresponding amplitude of the spectrum is lower than what is obtained with the TRM in the nearfield of the probe source.

In essence, the idea of the NTR focus, based on analytic continuation, is to combine the phase component $\exp(-i\mathbf{k} \cdot \mathbf{R}_1)$ of the spatial Fourier transform of the time-reversed field $\phi_{TR}(\mathbf{R}, \mathbf{R}_1, t)$ with the near-field shaping filter $\tilde{g}_S(\mathbf{k})$ of the generic analytic field $\phi_S(\mathbf{R}, \mathbf{R}_0, t)$, to construct $\tilde{\phi}_{NTR}(\mathbf{k}, \mathbf{R}_1, t)$, the spatial Fourier transform of the NTR field:

$$\tilde{\phi}_{NTR}(\mathbf{k}, \mathbf{R}_1, t) = A_S \exp(-i\mathbf{k} \cdot \mathbf{R}_1) \tilde{g}_S(\mathbf{k}) \exp(-i\omega t). \quad (8)$$

In physical space, the focus $\phi_{NTR}(\mathbf{R}, \mathbf{R}_1, t)$ is then

$$\phi_{NTR}(\mathbf{R}, \mathbf{R}_1, t) = A_S g_S(\mathbf{R}, \mathbf{R}_1) \exp(-i\omega t). \quad (9)$$

The NTR field $\phi_{NTR}(\mathbf{R}, \mathbf{R}_1, t)$ is constructed as follows when the localization phase is present for all k :

The phase for the position \mathbf{R}_1 of the focus from the TRM is obtained from $\tilde{\phi}_{TR}(\mathbf{k}, \mathbf{R}_1, t)$:

$$\exp(-i\mathbf{k} \cdot \mathbf{R}_1) = \frac{\tilde{\phi}_{TR}(\mathbf{k}, \mathbf{R}_1, t)}{|\tilde{\phi}_{TR}(\mathbf{k}, \mathbf{R}_1, t)|} \exp(i\omega t). \quad (10)$$

The spatial resolution $\tilde{g}_S(\mathbf{k})$ of the point source in the nearfield is obtained from $\tilde{\phi}_S(\mathbf{k}, \mathbf{R}_0, t)$, independently of the TRM and for *any* position \mathbf{R}_0 :

$$\tilde{g}_S(\mathbf{k}) = \frac{|\tilde{\phi}_S(\mathbf{k}, \mathbf{R}_0, t)|}{A_S}. \quad (11)$$

In practice, by substituting Eqs. (10) and (11) in (8), the spatial Fourier transform of the NTR field $\tilde{\phi}_{NTR}(\mathbf{k}, \mathbf{R}_1, t)$ is derived from $\tilde{\phi}_{TR}(\mathbf{k}, \mathbf{R}_1, t)$ and $\tilde{\phi}_S(\mathbf{k}, \mathbf{R}_0, t)$:

$$\tilde{\phi}_{NTR}(\mathbf{k}, \mathbf{R}_1, t) = \frac{\tilde{\phi}_{TR}(\mathbf{k}, \mathbf{R}_1, t)}{|\tilde{\phi}_{TR}(\mathbf{k}, \mathbf{R}_1, t)|} |\tilde{\phi}_S(\mathbf{k}, \mathbf{R}_0, t)|. \quad (12)$$

Hence, a high resolution focus is constructed from time reversal combined with components in the nearfield, with the latter actually representing any generic point source indepen-

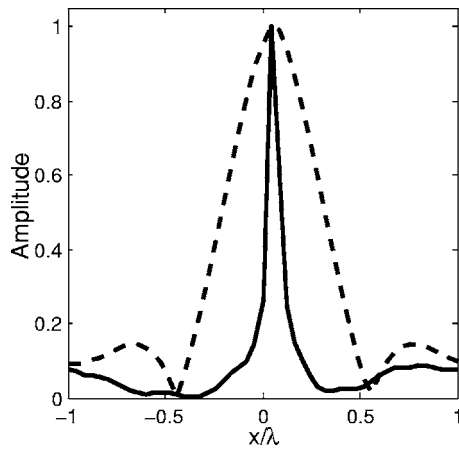


FIG. 1. Theoretical predictions for the normalized amplitude of the time-reversed field ϕ_{TR} from a TRM focusing at the center of the array (dark dashed line) and the resulting NTR ϕ_{NTR} (dark continuous line) obtained by combining ϕ_S with ϕ_{TR} following Eq. (12). The distance between the TRM and the probe source is $D=4\lambda$. The shaping filter $|g_s(\mathbf{R})| \approx \exp(-20k|\mathbf{R}|)$ was applied in this case. The different fields are generated within one wavelength and a $\lambda/25$ spatial sampling, for a 60-dB white noise relative to the maximum amplitude of ϕ_{TR} .

dent of the position of the original probe source. From a practical point of view, $|\tilde{\phi}_s(\mathbf{k}, \mathbf{R}_0, t)|$ is obtained from $\tilde{\phi}_s(\mathbf{R}, \mathbf{R}_0, t)$ with $|\mathbf{R}_0 - \mathbf{R}| < \lambda$. Increasing the number of elements of the near-field array within one wavelength will increase the focal resolution. It also has to be noted that, due to noise and other experimental limitations, in practice the shaping filter may not be obtained from $\phi_s(\mathbf{R}, \mathbf{R}_0, t)$, but generated numerically instead.

III. NUMERICAL SIMULATION

We first validate the NTR procedure using numerical computation, with added noise in anticipation of the experimental demonstration. The time-reversed field ϕ_{TR} is created on the near-field array using Eqs. (1)–(3), for either one source (Fig. 1) or two simultaneous sources separated by $\lambda/10$ (Fig. 2), with a TRM $D=4\lambda$ away from the probe source. The fields are generated within one wavelength with a $\lambda/25$ spatial sampling. A 60-dB white noise relative to the maximum amplitude is added for ϕ_{TR} . The NTR field ϕ_{NTR} is then obtained using Eq. (12) and a shaping filter defined with

$$|g_s(\mathbf{R})| \approx \exp(-20k|\mathbf{R}|). \quad (13)$$

Figure 1 shows the subwavelength focus for a single source. The spatial resolution of the focus corresponds to the one from the nearfield, with the position from the TRM. Figure 2 shows that each source is well separated from the other in ϕ_{NTR} , whereas that is not the case for the time-reversed field ϕ_{TR} . It has to be noted here that this result is not trivial since the operator in Eq. (12) is nonlinear with regard to the relative amplitudes; however, it is linear with regard to the phase of the superposition of the simultaneous sources.

IV. EXPERIMENTAL RESULTS

To confirm these results, an air acoustics experiment was conducted using loudspeakers and microphones between 100 and 200 Hz, as described in Figs. 3 and 4. For practical

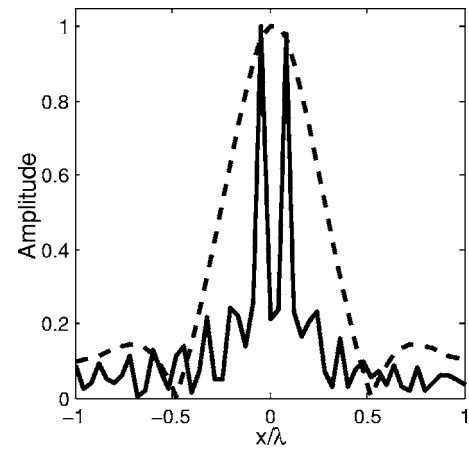


FIG. 2. Theoretical predictions for the normalized amplitude of the time-reversed field ϕ_{TR} from a TRM focusing simultaneously on two points separated by $\lambda/10$ (dark dashed line) and the resulting NTR ϕ_{NTR} (dark continuous line) obtained by combining ϕ_S with ϕ_{TR} following Eq. (12). The distance between the TRM and the probe source is $D=4\lambda$. The shaping filter $|g_s(\mathbf{R})| \approx \exp(-20k|\mathbf{R}|)$ was applied in this case. The different fields are generated within one wavelength and a $\lambda/25$ spatial sampling, with a 60-dB white noise relative to the maximum amplitude of ϕ_{TR} .

reasons, the experiment was done in a homogeneous free space medium. The TRM is composed of 24 speakers with a $\lambda/16$ spacing, corresponding to an aperture of $3\lambda/2$. The near-field array is composed of eight microphones with a $\lambda/47$ spacing. The arrays are linear and parallel to each other. The distance between the two arrays is $D=9$ m, corresponding to 4λ . The signal transmission and recording were done using a multichannel soundcard with a 40-dB signal-to-noise ratio. The impulse responses were recorded between each element of the TRM and each element of the near-field array. The time-reversed field ϕ_{TR} was generated from a digital time-reversal experiment by correlating the recorded im-

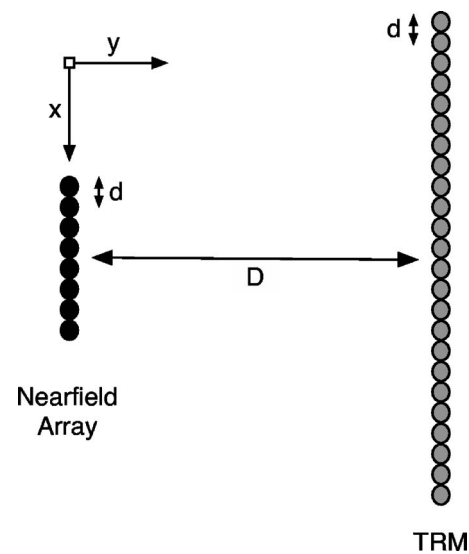


FIG. 3. Experimental setup used in the audible range from 100 to 200 Hz ($\lambda=2.3$ m, not to scale). The TRM (gray) consists in a linear array composed of 24 speakers with a $\lambda/16$ spacing. The near-field array (black) is a linear array composed of eight microphones with a $\lambda/47$ spacing. The distance between the two arrays is $D=9$ m, $D \approx 4\lambda$. The signal transmission and recording was done using a multichannel soundcard with a 40-dB signal-to-noise ratio.

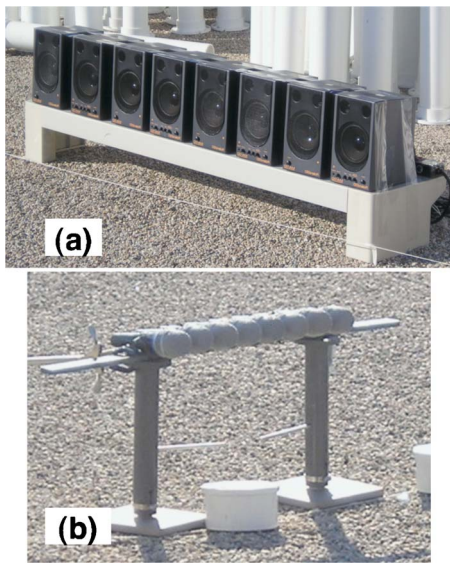


FIG. 4. (Color online) (a) Time-reversal mirror (TRM) composed of eight loudspeakers (Roland MA110). The 24-element TRM was obtained by moving the eight elements three times. (b) Near-field array composed of eight microphones (Shure PG57). Both arrays are connected to a Aardvark Direct Pro Q10 10 channels sound card and controlled by a PC computer.

pulse responses between all the elements of the TRM and the near-field array with the ones from the TRM to the desired focus.

To account for the experimental conditions, g_s was defined for this experiment with an exponential relative to the element 4 on the array instead of the theoretical target field from Eq. (1), using

$$|g_s(\mathbf{R}, \mathbf{R}_4)| \approx \exp(-5k|\mathbf{R} - \mathbf{R}_4|), \quad (14)$$

where $k=2\pi f/c$, with $c=350 \text{ m s}^{-1}$ and $f=150 \text{ Hz}$. The coefficient 5 in the exponential was chosen empirically for this experiment as a compromise between the main and side lobes of the resulting NTR focus. The time-reversed field ϕ_{TR} from the far-field TRM is recorded on the near-field array elements. The focus associated with ϕ_{TR} for a single focus under the experimental conditions corresponded to about $8\lambda/3$ at the 50% downpoints [Fig. 5(a)], corresponding to the size of the focus one might expect with a distance $D=4\lambda$ between the focus and a TRM with a $3\lambda/2$ aperture. Using the same 50% downpoints criterion, NTR achieves a $\lambda/20$ focus for a single focusing position [Fig. 5(a)]. This subwavelength focusing is of the same order as the ones reported for NAH^{10,11} and smaller than that by de Rosny and Fink.⁹ They obtained a $\lambda/14$ spatial resolution experimentally in a cavity, which was most likely limited by the timing and amplitude adjustments of the time-reversed source field they applied at the source to compensate the outgoing field.⁹ Experimental results with a larger spacing for the near-field array showed that the NTR focus was broader. In the case of two foci occurring simultaneously on two elements (3 and 5) of the near-field array separated by one element (4) only, i.e., separated by $\lambda/23$, the improvement observed on each focus compares well to theoretical predictions [Fig. 5(b)]. This result is obtained without loss on the

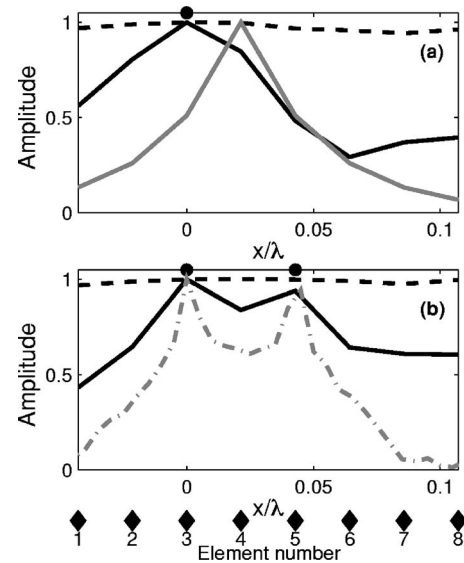


FIG. 5. (a) Experimental results in the audible range from 100 to 200 Hz ($f=150 \text{ Hz}$, $c=350 \text{ ms}^{-1}$, $\lambda=2.3 \text{ m}$, $D \approx 4\lambda$) for the time-reversed field ϕ_{TR} (dark dashed line), the theoretically derived point source field $\phi_s(\mathbf{R}, \mathbf{R}_4, t)$ (light continuous line), and the NTR field ϕ_{NTR} (dark continuous line) in the case of focusing on one element (dark point) of the near-field array. Subwavelength resolution of $\lambda/20$ to 50% down in amplitude is obtained. (b) Experimental results from 100 to 200 Hz ($\lambda=2.3 \text{ m}$) for the time-reversed field ϕ_{TR} (dark dashed line) and NTR ϕ_{NTR} (dark continuous line) fields when two foci occur simultaneously on the elements 3 and 5 (dark points, $\lambda/23$ apart) of the eight-element near-field array. Also shown, the theoretical predictions for the NTR with two sources $\lambda/23$ distant for a 40-dB white noise and $\lambda/200$ spatial resolution of the array (light dash-dotted line).

temporal resolution of each focus. A focus can be transmitted to different positions of the near-field array independently of the others, within the limitations of the experimental conditions.

V. CONCLUSION

In this paper, we demonstrated using theory and experiments that subwavelength focusing with time reversal is achieved without *a priori* knowledge on the original source and away from the nearfield of the probe source, as opposed to the acoustic sink procedure or NAH. This result is obtained by combining near-field and TRM components in the wave-number space following the NTR principles, within the limitation in range presented. Interestingly, the subwavelength focusing is obtained without loss of the temporal resolution. This technique is applied to an array with elements within a fraction of the wavelength from each other, using the knowledge of their relative positions only. Potentially, this technique can be used to enhance NAH imaging and increase the range between the NAH array and the sample to image. NTR also allows focusing different signals simultaneously on different elements within a fraction of a wavelength of each other, a goal very basic to construct multi-channel communications techniques.

ACKNOWLEDGMENTS

The authors would like to acknowledge the valuable discussions with Mathias Fink.

- ¹M. Fink, "Time reversed acoustics," *Phys. Today* **50**(3), 34–40 (1997).
- ²B. Y. Zel'dovitch, N. F. Pilipetsky, and V. V. Shkunov, in *Principles of Phase Conjugation* (Springer Verlag, Berlin, 1985).
- ³G. Lerosey, J. de Rosny, A. Tourin, A. Derode, G. Montaldo, and M. Fink, "Time reversal of electromagnetic waves," *Phys. Rev. Lett.* **92**, 193904 (2004).
- ⁴G. Lerosey, J. de Rosny, A. Tourin, A. Derode, G. Montaldo, and M. Fink, "Time reversal of electromagnetic waves and telecommunication," *Radio Sci.* **40**, RS6S12 (2005).
- ⁵D. Cassereau and M. Fink, "Time reversal of ultrasonic fields—Part I: Basic principles," *IEEE Trans. Ultrason. Ferroelectr. Freq. Control* **39**, 579 (1992).
- ⁶P. Blomgren, G. Papanicolaou, and H. Zhao, "Super-resolution in time-reversal," *J. Acoust. Soc. Am.* **111**, 230–248 (2002).
- ⁷D. R. Jackson and D. R. Dowling, "Phase conjugation in underwater acoustics," *J. Acoust. Soc. Am.* **89**, 171–181 (1991).
- ⁸A. Derode, P. Roux, and M. Fink, "Robust acoustic time reversal with high-order multiple scattering," *Phys. Rev. Lett.* **75**(23), 4206–4209 (1995).
- ⁹J. de Rosny and M. Fink, "Overcoming the diffraction limit in wave physics using a time-reversal mirror and a novel acoustic sink," *Phys. Rev. Lett.* **89**, 124301 (2002).
- ¹⁰E. G. Williams and J. D. Maynard, "Holographic imaging without the wavelength resolution limit," *Phys. Rev. Lett.* **45**(7), 554–557 (1980).
- ¹¹J. D. Maynard, E. G. Williams, and Y. Lee, "Nearfield acoustic holography: I. Theory of generalized holography and the development of NAH," *J. Acoust. Soc. Am.* **78**, 1395–1413 (1985).